A mathematical model for drying paint layers

S. D. HOWISON[2], J. A. MORIARTY[3], J. R. OCKENDON[2], E. L. TERRILL[4] and
S. K. WILSON[1]
[1] *Department of Mathematics, University of Strathclyde, Livingstone Tower, 26 Richmond Street, Glasgow G1
1XH, UK (e-mail: s.k.wilson@strath.ac.uk)*[1]
[2] *Oxford Centre for Industrial and Applied Mathematics, Mathematical Institute, 24-29 St. Giles', Oxford OX1
3LB, UK*
[3] *Advanced Engineering Design Center, Baxter Healthcare, Route 120 and Wilson Road, Round Lake, IL 60073,
USA*
[4] *Faculty of Mathematical Studies, University of Southampton, Southampton S09 5NH, UK*

Abstract. Many industrial processes involve the coating of substrates with thin layers of paint. This paper is concerned with modelling the variations in layer thickness which may occur as a paint layer dries. Firstly, a systematic derivation is provided of a model based on classical lubrication theory for a drying paint layer consisting of a non-volatile resin and a volatile solvent. The effects of variable surface tension, viscosity, solvent diffusivity and solvent evaporation rate are all included in the model. This analysis makes explicit the validity of the physically intuitive approximations made by earlier authors and hence clarifies when the model is appropriate. Secondly, the model is used to analyse the evolution of small perturbations to the thickness of, and the concentration of solvent in, a drying paint layer. This analysis provides an analytical description of the 'reversal' of an initial perturbation to the thickness of the layer and the appearance of a perturbation to an initially flat layer caused by an initial perturbation to the concentration of solvent. Thirdly, it is shown how a simplified version of the model applicable to the case of surface-tension-gradient-dominated flow can be derived and solved as an initial-value problem. Fourthly, the applicability of the present theory developed for solvent-based high-gloss alkyd paints to waterborne coatings is discussed. Finally, the results obtained are summarised and the practical implications of the work are discussed.

Key words: mathematical modelling, thin viscous films, surface-tension gradients, paints, coatings.

1. Introduction

Many industrial processes involve the coating of substrates with thin layers of paint. In this paper we model the variations in the thickness of the layer which may occur as a paint layer dries. Typically, as a layer of paint dries, any non-uniformities in the inital layer thickness die out under the action of constant surface tension, eventually leaving a layer of almost uniform thickness. This levelling motion is described in the early work of Smith, Orchard and Rhind-Tutt [1] and Orchard [2]. However, the experiments described by Overdiep [3, 4] show that some solvent-based high-gloss alkyd paints can exhibit more unusual behaviour as they dry. Firstly, the experiments showed an initially faster rate of levelling than that expected due simply to constant surface-tension effects. Secondly, and much more unexpectedly, after several minutes the paint surface underwent 'reversal'; that is, the original peaks became troughs and the original troughs became peaks. Recent experiments by Kojima, Moriga and Takenouchi [5, 6] show the same behaviour in waterborne coatings with high volatility (compared to water) co-solvent. Overdiep [3, 4] was the first to suggest that the presence of surface tension gradients might provide an explanation for both these phenomena. As

---

[1] Author for correspondence.

Kornum and Raaschou Nielsen [7] describe, solvent-based high-gloss alkyd paints consist of a non-volatile resin dissolved in a volatile solvent. Since the surface tension of pure resin is higher than that of pure solvent, the surface tension of the layer is a decreasing function of the local concentration of solvent. As the solvent evaporates and the layer begins to level under the action of an initially uniform surface-tension force, the concentration of solvent near the peaks relative to the concentration near the troughs increases and hence the surface tension at the peaks becomes lower than that at the troughs. The resulting gradient of surface tension drives a flow from the peaks to the troughs which enhances the levelling process. The imbalance in the concentration of solvent is still present when the paint surface becomes level, and so surface-tension gradients continue to drive the flow and cause the observed reversal. The phenomena described above are caused by initial non-uniformities in the layer thickness. However, any initial non-uniformities in solvent concentration will also drive a flow which will produce non-uniformities in the thickness of even an initially flat layer.

Overdiep [3, 4] proposed a simple yet effective model for a drying paint layer which included the effect of variable surface tension caused by non-uniformities in the concentration of solvent and was capable of reproducing the observed reversal. This model has been analysed and generalised by Wilson [8], Moriarty, Terrill and Wilson [9] and Schwartz and Eley [10], who found good agreement between analytical and numerical calculations made, using the model and the experimental results for a planar substrate. The extension of the model to include the effects of a curved substrate has recently been investigated by Weidner, Schwartz and Eley [11]. The general problem of flow in thin liquid films driven by surface tension and surface-tension gradients has been studied by many different authors in a variety of other physical contexts. Among these Burelbach, Bankoff and Davis [12] investigated the stability and possible rupture of evaporating and condensing films accounting for vapour recoil, thermocapillary and van-der-Waals effects, while Jensen and Grotberg [13, 14] analysed the spreading of both insoluble and soluble surfactant on thin films and De Wit, Gallez and Christov [15] investigated the dynamics of thin free films with insoluble surfactants.

In this paper we begin in Section 2 by providing a systematic derivation of a generalisation of Overdiep's [3, 4] mathematical model based on classical lubrication theory for a drying paint layer consisting of a non-volatile resin and a volatile solvent. The effects of variable surface tension, viscosity, solvent diffusivity and solvent evaporation rate are all included in the model. This analysis makes explicit the validity of the physically intuitive approximations made by earlier authors and hence clarifies when the model is appropriate. In Section 3 we use the model to analyse the evolution of small perturbations to the thickness of, and the concentration of solvent in, a drying paint layer. This analysis provides an analytical description of the reversal of an initial perturbation to the thickness of the layer and the appearance of a perturbation to an initially flat layer caused by an initial perturbation to the concentration of solvent. In Section 4 we show how a simplified version of the model applicable to the case of surface-tension-gradient-dominated flow can be derived and solved as an initial-value problem. In Section 5 we discuss the applicability of the present theory developed for solvent-based high-gloss alkyd paints to waterborne coatings. Finally, in Section 6 we summarise the results obtained and discuss the practical implications of the work.

2.   Derivation of the model

We consider a two-dimensional situation in which the horizontal and vertical co-ordinates are denoted by x and y, respectively; with respect to these co-ordinates and to time, t, the free

Table 1. Relevant parameters and their typical magnitudes for solvent-based high-gloss alkyd paint taken from Overdiep [4] (Paint B) $(\tau_s, \tau_r, S_0, M_0, E_0, \rho, H, L)$ and van der Hout [16] (D_0).

Parameter	Symbol	Value	Units
Surface tension of pure solvent	τ_s	$2\cdot3 \times 10^{-2}$	Nm^{-1}
Surface tension of pure resin	τ_r	$3\cdot1 \times 10^{-2}$	Nm^{-1}
Initial concentration of solvent	S_0	$0\cdot5$	–
Initial viscosity of paint	M_0	$0\cdot55$	$\mathrm{Nm}^{-2}\mathrm{s}$
Initial evaporation rate of solvent	E_0	$\simeq 10^{-8}$	ms^{-1}
Initial diffusivity of solvent	D_0	$\simeq 10^{-8}$	$\mathrm{m}^2\mathrm{s}^{-1}$
Density of paint	ρ	$\simeq 10^3$	$\mathrm{kg\,m}^{-3}$
Characteristic layer thickness	H	$6\cdot0 \times 10^{-5}$	m
Characteristic horizontal length	L	$4\cdot0 \times 10^{-3}$	m

surface of the paint is given by $y = h(x, t)$. We assume that both the density of resin and the density of solvent are equal to the constant paint density ρ and denote the total flux of the paint by $\boldsymbol{q} = (\rho u, \rho v) = \boldsymbol{q}_r + \boldsymbol{q}_s$, which comprises the resin flux, $\boldsymbol{q}_r$, and the solvent flux, $\boldsymbol{q}_s$. We model the paint as a Newtonian fluid with variable viscosity, and so use the Navier-Stokes equations. The surface tension of the paint, $\tau = \tau(s)$, is assumed to be a linear function of the solvent volume fraction (concentration), s, so that $\tau(s) = \tau_r - s\Delta\tau$, where $\Delta\tau = \tau_r - \tau_s > 0$ is the difference between the surface tension of pure resin, τ_r, and that of pure solvent, τ_s. The viscosity of the paint, $\mu = \mu(s)$, is assumed to depend on the solvent concentration only. We denote the acceleration due to gravity by g and assume that the pressure in the passive gas above the paint layer is zero. The relevant parameters and their typical magnitudes are listed in Table 1. The characteristic lengths may vary from experiment to experiment, and the values given here for L and H are the wavelength of initial perturbations to the layer thickness and the initial mean thickness of the layer, respectively, in Overdiep's [4] experiments. Note that Overdiep [3, 4] suggests that the solvent evaporation rate is approximately constant over the timescales we are considering. Typically, the solvent diffusivity is a strongly varying function which may change by several orders of magnitude as the solvent concentration varies. The value given in Table 1 is a typical one taken from data supplied to us by van der Hout [16].

In the derivation of the model which follows we allow both the solvent evaporation rate, $E_0 e(s)$, and solvent diffusivity, $D_0 d(s)$, to depend on the solvent concentration. We assume that the solvent flux consists of a term due to the bulk flow and a diffusive term so that $\boldsymbol{q}_s = s\boldsymbol{q} - \rho D_0 d\boldsymbol{\nabla}s$, and hence the equation governing the flow of solvent in the paint layer is

$$\rho s_t + \boldsymbol{q} \cdot \boldsymbol{\nabla}s = \rho D_0 \nabla \cdot (d\nabla s). \tag{1}$$

On the substrate, $y = 0$, the resin and solvent fluxes are zero. On the free surface, $y = h$, the normal and tangential components of stress are both continuous, and the kinematic conditions for the resin and solvent are

$$\boldsymbol{q}_r \cdot \boldsymbol{n} = \rho(1 - s)v_n, \qquad \boldsymbol{q}_s \cdot \boldsymbol{n} = \rho(sv_n + E_0 e),$$

respectively, where $\boldsymbol{n}$ is the unit outward normal to the free surface and v_n is the speed of the free surface in that direction.

We intend to non-dimensionalise the equations and boundary conditions in the usual way by scaling x with L, y with H, t with L/U, u with U, v with UH/L, h with H, s with S (a characteristic measure of the variation in s over the horizontal lengthscale L), μ with M_0 and τ with τ_r. Then we shall exploit the smallness of the non-dimensional aspect ratio of the layer, $\epsilon = H/L$, to simplify the problem, using the familiar lubrication approximation. However, before we can do this, we need to establish the appropriate characteristic horizontal speed, U, which is not known *a priori*, but is determined by the dominant physical mechanism driving the flow. There are two extreme cases, namely flow driven purely by mean surface-tension forces and flow driven purely by surface-tension-gradient forces. For flow driven by mean surface-tension forces, U is given by balancing the viscous force with the mean surface-tension force in the normal-stress condition, and so $U = U_s = \epsilon^3 \tau_r / M_0$. Alternatively, for flow driven by surface-tension-gradient forces, U is given by balancing the viscous force with the surface-tension-gradient force in the tangential-stress condition, and so $U = U_g = \epsilon S \Delta \tau / M_0$. The ratio of these two velocity scales is $U_g/U_s = S \Delta \tau / \epsilon^2 \tau_r$, and we are particularly interested in situations in which this ratio is $O(1)$ as $\epsilon \to 0$, *i.e.* situations in which U_s and U_g are comparable.

Two such situations are immediately apparent. In the first case, the variation of surface tension with $O(1)$ changes in the solvent concentration, $\Delta \tau / \tau_r$, is $O(1)$, but changes in the solvent concentration, S, are only $O(\epsilon^2)$. This situation is typical of the evolution of a paint layer with an initially uniform solvent concentration. In the second case, the variation of surface tension with $O(1)$ changes in the solvent concentration is only $O(\epsilon^2)$, but now changes in the solvent concentration are $O(1)$.

If $U_g/U_s \gg 1$, then the flow is driven by surface-tension-gradient forces; this situation is treated in Section 4. If $U_g/U_s \ll 1$, we recover the familiar situation in which the flow is driven by mean surface-tension forces.

Using the values of the parameters given in Table 1, we obtain $U_s = 1 \cdot 9 \times 10^{-7} \, \mathrm{m \, s^{-1}}$ with corresponding typical timescale $T_s = L/U_s = 2 \cdot 1 \times 10^4 \, \mathrm{s}$, while, taking $S = 1$, we have $U_g = 2 \cdot 2 \times 10^{-4} \, \mathrm{m \, s^{-1}}$, which is much faster than U_s, and $T_g = L/U_g = 18 \, \mathrm{s}$, which is correspondingly shorter than T_s. Overdiep's [3, 4] experimental results indicate that for the reversal problem the real situation is rather more complicated than either of these two limiting cases suggests; they show that the timescale for the reversal of the perturbation to the layer profile is roughly $T_e = 10^2 \, \mathrm{s}$, which lies between T_s and T_g, with a corresponding value of $U_e = L/T_e = 4 \cdot 0 \times 10^{-5} \, \mathrm{m \, s^{-1}}$. The explanation for this 'intermediate' timescale is that, initially, concentration- and, hence, surface-tension gradients are absent (*i.e.* $S = 0$) and mean surface-tension forces are dominant, but that the evaporation of solvent generates gradients in the solvent concentration (so that S increases) and hence in the surface tension, which eventually becomes the dominant mechanism driving the flow.

Non-dimensionalising the equations and boundary conditions as indicated above introduces, in addition to the aspect ratio, a reduced Reynolds number $R = \rho U L \epsilon^2 / M_0$, non-dimensional diffusion coefficient (inverse Péclet number) $D = D_0/LU$ and evaporation coefficient $E = E_0/\epsilon U$, inverse capillary number $C = \epsilon^3 \tau_r / M_0 U$, Marangoni number $M = \epsilon S \Delta \tau / M_0 U$ and Bond number $B = \epsilon^3 \rho g L^2 / M_0 U$. Typical values of the parameters R, D, E, C, M and B with $U = U_s, U_g$ and U_e are given in Table 2. Note that, in order to calculate these values, we took $S = \epsilon^2$ in the first case and $S = 1$ in the last two. Typically, ϵ is small and so, as indicated earlier, we treat the problem in the asymptotic limit $\epsilon \to 0$. Motivated by the magnitudes of the parameters given in Table 2, we choose to include the effects of evaporation, mean surface tension, surface-tension gradients and gravity in the lead-

ing order problem, but neglect those of inertia. Thus, we assume that E, C, M and B are all $O(1)$, but that $R = o(1)$ as $\epsilon \to 0$. The size of D is left unspecified for the present. Thence the leading-order velocity (u_0, v_0), pressure p_0 and viscosity μ_0 satisfy the equations of classical lubrication theory:

$$u_{0x} + v_{0y} = 0, \tag{2}$$

$$p_{0x} = (\mu_0 u_{0y})_y, \tag{3}$$

$$p_{0y} = -B. \tag{4}$$

On the substrate, $y = 0$, the leading-order boundary conditions on the flux are simply

$$u_0 = v_0 = 0. \tag{5}$$

On the free surface, $y = h_0$, the leading-order versions of the normal[1] and tangential force balance conditions are

$$-p_0 = Ch_{0xx}, \tag{6}$$

$$\mu_0 u_{0y} = -M(s_{0x} + h_{0x}s_{0y}). \tag{7}$$

At leading order the kinematic condition for the paint (simply a statement of conservation of mass of paint) can be written

$$h_{0t} + Q_{0x} = -Ee_0, \tag{8}$$

where $e_0 = e(s_0)$ and Q_0 is the leading-order horizontal volume flux. Provided that $\epsilon^2/D = o(1)$ as $\epsilon \to 0$, the leading-order version of (1) is simply

$$(d_0 s_{0y})_y = 0,$$

where $d_0 = d(s_0)$. At leading order the boundary conditions for the solvent concentration reduce to $s_{0y} = 0$ on $y = 0$ and $y = h$ and so we can deduce at once that $s_0 = s_0(x, t)$, *i.e.* the diffusion of solvent is sufficiently rapid to make the leading-order distribution of solvent uniform or 'well-mixed' across the layer. The leading-order pressure is determined from (4) and (6). Since s_0, and hence μ_0, are independent of y, we can solve (3) subject to the boundary conditions (5) and (7) for u_0 and hence obtain

$$Q_0 = \frac{h_0^3}{3\mu_0}(Ch_{0xx} - Bh_0)_x - \frac{h_0^2}{2\mu_0}Ms_{0x}. \tag{9}$$

To determine s_0 we need to proceed to next order in the asymptotic analysis. If $D \sim 1$, lateral diffusion of solvent is comparable with convection and we seek a solution in the form $s(x, y, t) = s_0(x, t) + \epsilon^2 s_1(x, y, t) + o(\epsilon^2)$ where s_1 satisfies

$$s_{0t} + u_0 s_{0x} = D(d_0 s_{0x})_x + D(d_0 s_{1y})_y,$$

subject to the boundary conditions $s_{1y} = 0$ on $y = 0$ and

$$Dd_0 s_{1y} = -Ee_0(1 - s_0) + Dd_0 h_{0x} s_{0x}$$

Table 2. Typical values of the parameters with $U = U_s, U_g$ and U_e. Note that $S = \epsilon^2$ in the first case and $S = 1$ in the last two.

	$U = U_s$	$U = U_g$	$U = U_e$
R	$3 \cdot 1 \times 10^{-10}$	$3 \cdot 6 \times 10^{-7}$	$6 \cdot 5 \times 10^{-8}$
D	13	$1 \cdot 1 \times 10^{-2}$	$6 \cdot 2 \times 10^{-2}$
E	$3 \cdot 5$	$3 \cdot 1 \times 10^{-3}$	$1 \cdot 7 \times 10^{-2}$
C	1	$8 \cdot 7 \times 10^{-4}$	$4 \cdot 8 \times 10^{-3}$
M	$0 \cdot 26$	1	$5 \cdot 4$
B	$5 \cdot 1$	$4 \cdot 4 \times 10^{-3}$	$2 \cdot 4 \times 10^{-2}$

on $y = h_0$. So, using (8), we obtain the equation

$$(h_0 s_0)_t + (Q_0 s_0)_x = -E e_0 + D(d_0 h_0 s_{0x})_x, \tag{10}$$

which is simply a statement of conservation of mass of solvent. Note that the corresponding statement of conservation of mass of resin can be obtained explicitly by an appropriate combination of (8) and (10).

Equations (8) and (10), together with the definition of Q given by Equation (9), represent a generalisation of the model suggested by Overdiep [4], extended to include the effects of variable solvent evaporation rate and solvent diffusivity. If $\epsilon^2 \ll D \ll 1$, lateral diffusion of solvent is dominated by convection and a similar argument leads to

$$(h_0 s_0)_t + (Q_0 s_0)_x = -E e_0 \tag{11}$$

instead of (10), and so we recover the model described by Overdiep [3] which neglects the effects of lateral diffusion. If $D \gg 1$, lateral diffusion of solvent dominates convection and so the convective timescale L/U is no longer appropriate and must be replaced with the shorter diffusive timescale $L^2/D_0 = L/UD$. Rescaling t appropriately, we find that, at leading order, Equation (8) is just $h_{0t} = 0$, while the appropriate version of (10) is simply

$$(h_0 s_0)_t = (h_0 s_{0x})_x.$$

Since the free surface remains stationary on this shorter timescale over which rapid diffusion occurs, we shall not pursue this case further here. (Note that in this case we require that $DR = o(1)$ as $\epsilon \to 0$ in order to neglect the unsteady terms in the governing equations.) If the condition $D \gg \epsilon^2$ fails to hold, the leading-order distribution of solvent across the layer is no longer uniform and the model becomes more unwieldy as a result. For example, if $D = \hat{D}\epsilon^2$ as $\epsilon \to 0$, the leading-order version of (1) is

$$s_{0t} + u_0 s_{0x} + v_0 s_{0y} = \hat{D}(d_0 s_{0y})_y.$$

As a consequence s_0, and therefore d_0, e_0 and μ_0 are now in general functions of y as well as x and t, and so the corresponding expression for Q_0 is more complicated than that obtained previously.

Hereafter we drop the zero subscript and all quantities correspond to their leading-order terms in the limit $\epsilon \to 0$.

3. Evolution of small perturbations to a drying paint layer

In this section we examine the evolution of small perturbations to the thickness of, and the concentration of solvent in, a drying paint layer. For simplicity we take $d_0 = e_0 \equiv 1$ and seek solutions in the form

$$h(x,t) = h_0(t) + h_1(t)\, e^{i\alpha x}, \qquad s(x,t) = s_0(t) + s_1(t)\, e^{i\alpha x},$$

where

$$h_0(t) = 1 - Et, \qquad s_0(t) = \frac{S_0 - Et}{1 - Et},$$

subject to the general initial conditions $h_1(0) = H_1$ and $s_1(0) = S_1$. The basic state described by h_0 and s_0 represents a decrease in the uniform thickness of the layer and in the concentration of solvent caused by the uniform evaporation of solvent. Evidently, this solution is valid only when $t < S_0/E$. This restriction is a consequence of the assumption that the evaporation rate is constant and can easily be removed if a more realistic choice of e_0 is made (see [8]). However, the timescale over which the reversal occurs is typically much shorter than S_0/E and so taking $e_0 \equiv 1$ is sufficient for the present purpose. The first-order versions of Equations (8) and (10) can be solved exactly to yield an explicit expression for the solvent perturbation,

$$s_1(t) = \frac{1}{h_0}\left[S_1 + E(1 - S_0) \int_0^t \frac{h_1(\hat{t})}{h_0^2(\hat{t})}\, e^{\alpha^2 D \hat{t}}\, \mathrm{d}\hat{t} \right] e^{-\alpha^2 D t}. \tag{12}$$

Hence we obtain an integro-differential equation with non-constant coefficients for the perturbation to the thickness of the layer $h_1(t)$,

$$h_{1t} + \frac{\sigma h_0^3}{\mu_0} h_1 + \frac{\gamma h_0}{\mu_0}\left[S_1 + E(1 - S_0) \int_0^t \frac{h_1(\hat{t})}{h_0^2(\hat{t})}\, e^{\alpha^2 D \hat{t}}\, \mathrm{d}\hat{t} \right] e^{-\alpha^2 D t} = 0, \tag{13}$$

where $\mu_0 = \mu(s_0)$ and $\sigma = \alpha^2(\alpha^2 C + B)/3$ and $\gamma = \alpha^2 M/2$ are both constants; (13) is subject to the initial condition $h_1(0) = H_1$. Note that the constant $\sigma > 0$ is simply the exponential decay rate obtained by Orchard [2] in the absence of surface-tension-gradient effects $(\gamma = 0)$.

The integro-differential equation (13) can also be written as a linear second-order differential equation for the new independent variable

$$F(t) = \int_0^t \frac{h_1(\hat{t})}{h_0^2(\hat{t})} e^{\alpha^2 D \hat{t}}\, \mathrm{d}\hat{t},$$

in the form

$$\frac{\mathrm{d}^2 F}{\mathrm{d}t^2} + f(t)\frac{\mathrm{d}F}{\mathrm{d}t} + g(t)F + h(t) = 0 \tag{14}$$

where

$$f(t) = \frac{\sigma h_0^3}{\mu_0} - \frac{2E}{h_0} - \alpha^2 D, \quad g(t) = \frac{\gamma E(1 - S_0)}{h_0 \mu_0}, \quad h(t) = \frac{\gamma S_1}{h_0 \mu_0},$$

subject to the initial conditions $F = 0$ and $\mathrm{d}F/\mathrm{d}t = H_1$ at $t = 0$. Once F has been determined, h_1 and s_1 can be calculated from the expressions

$$h_1(t) = h_0^2(t) \frac{\mathrm{d}F}{\mathrm{d}t} \mathrm{e}^{-\alpha^2 Dt}, \quad s_1(t) = \frac{S_1 + E(1 - S_0)F(t)}{h_0(t)} \mathrm{e}^{-\alpha^2 Dt}. \tag{15}$$

We solved Equation (14) analytically in the asymptotic limit of small evaporation rate $E \to 0$ and numerically with a Runge-Kutta-Merson method using NAG routine D02BBF.

Details of the asymptotic solution are given in the Appendix. In particular, this analysis shows that, if $\epsilon^2 \ll D \ll 1$ and $S_1 = 0$, then, as t becomes large, the first-order perturbation to the thickness of the layer approaches the limiting value

$$-\frac{9M(1 - S_0)H_1 E}{2\alpha^2(\alpha^2 C + B)^2}, \tag{16}$$

where the minus sign represents the reversal of the initial perturbation to the free surface, and the first-order perturbation to the solvent concentration approaches the limiting value

$$\frac{3(1 - S_0)H_1 E}{\alpha^2(\alpha^2 C + B)}. \tag{17}$$

These results generalise the corresponding expressions given in [8] for the special case $B = 0$. Alternatively, if $S_1 \neq 0$, then, as t becomes large, the first-order perturbations ultimately both grow linearly in time and eventually they become so large that the asymptotic analysis ceases to apply.

In order to perform the present numerical calculations we took the function $\mu = \mu(s)$ to be $\mu(s) = \exp(-M_1(s - S_0))$, where we found the value of M_1 by equating the leading-order term in the expansion of $\mu(s)$ in powers of $E \ll 1$ with the exponential fit for the viscosity involving the empirically determined constant t_k given in [4], to yield $M_1 = L/E(1 - S_0)Ut_k$. Adopting the surface-tension-gradient scaling with $S = 1$ and taking $t_k = 270$, we obtain $M_1 \simeq 44$. Numerically-calculated and asymptotic values of $h_1(t)$ and $s_1(t)$ are plotted as functions of t, using the values of the parameters given in Table 1 in the case $\epsilon^2 \ll D \ll 1$ in Figures 1 and 2 using the initial conditions $H_1 \neq 0$, $S_1 = 0$ and $H_1 = 0$, $S_1 \neq 0$, respectively. As expected, both show good agreement between the numerical calculations and the asymptotic theory provided that $t \ll 1/EM_1(1 - S_0) \simeq 15$. Figure 1(a) clearly shows the initial levelling and eventual reversal of an initial perturbation to the thickness of the layer and Figure 1(b) shows the corresponding development of a non-uniform perturbation to the initially-uniform solvent concentration. In particular, Figure 1(a) shows that the free surface becomes flat for the first time at dimensionless time $t \simeq 6$ (corresponding to roughly 10^2 seconds, in agreement with the experimental results). Numerical solutions of Equation (14) for other parameter values (such as those described in [8]) show that the free surface may reverse several times in an oscillatory manner as the paint dries. In the absence of evaporation the free surface just levels exponentially in time and the solvent concentration remains constant. Figure 2 shows that an
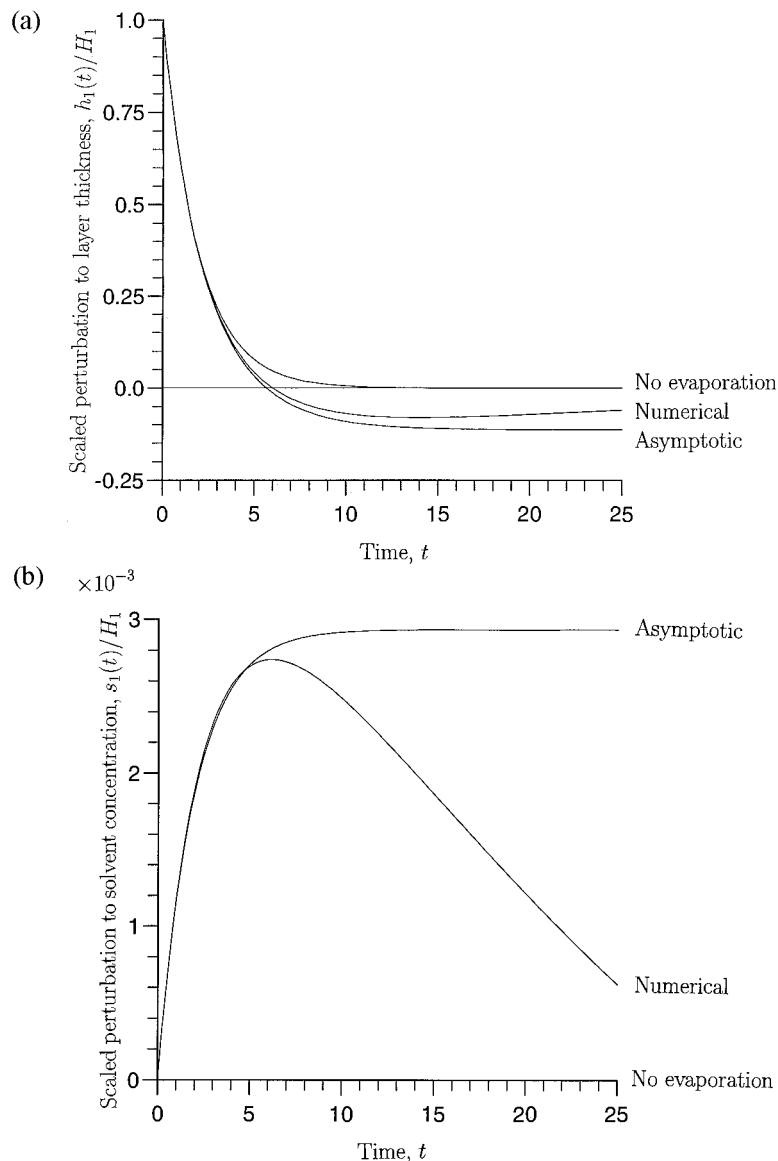
Figure 1. Numerically-calculated and asymptotic values of the perturbations to (a) the scaled layer thickness $h_1(t)/H_1$ and (b) the scaled solvent concentration $s_1(t)/H_1$, both plotted as functions of time t with the values of the parameters given in Table 1 in the case $H_1 \neq 0$, $S_1 = 0$. The corresponding exact solutions in the case of no evaporation, $E = 0$, are also shown.

initial perturbation to the solvent concentration produces a perturbation to the free surface profile of an initially flat layer. This occurs even in the absence of evaporation, in which case the perturbation to the free surface ultimately has amplitude $-3MS_1/2(\alpha^2 C + B) \simeq -44S_1$.

4. Surface-tension-gradient-dominated flow

In this section we investigate the situation $U_g/U_s = M/C \gg 1$ in which the flow is dominated by surface-tension-gradient effects. For simplicity, we investigate the case $\epsilon^2 \ll D \ll 1$ and
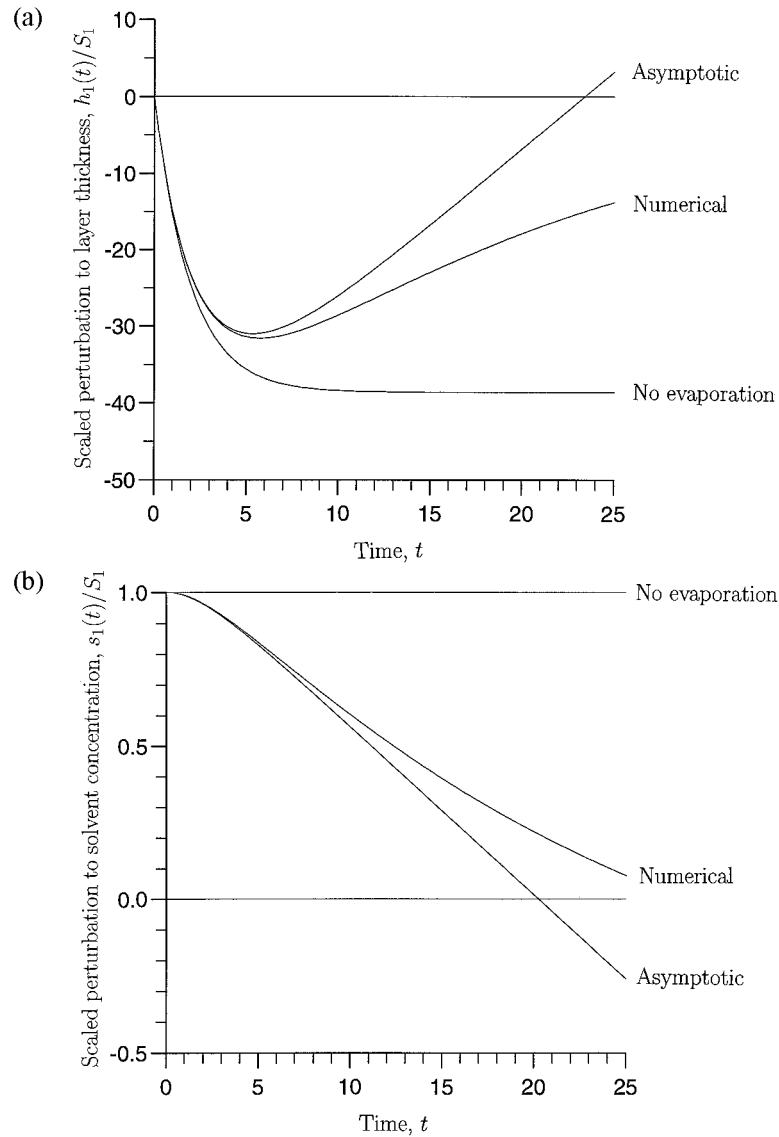
Figure 2. Numerically-calculated and asymptotic values of the perturbations to (a) the scaled layer thickness $h_1(t)/S_1$ and (b) the scaled solvent concentration $s_1(t)/S_1$, both plotted as functions of time t with the values of the parameters given in Table 1 in the case $H_1 = 0$, $S_1 \neq 0$. The corresponding exact solutions in the case of no evaporation, $E = 0$, are also shown.

neglect the effects of solvent evaporation and of gravity. Adopting the surface-tension-gradient scaling, a derivation similar to that presented in Section 2 yields the model equations

$$h_t - \left(\frac{h^2 s_x}{2\mu} \right)_x = 0, \qquad s_t - \frac{h s_x^2}{2\mu} = 0. \tag{18}$$

Hence, h is given by

$$h = \frac{2\mu s_t}{s_x^2}, \tag{19}$$

where s satisfies the quasi-linear second-order hyperbolic equation

$$3s_t^2 s_{xx} - 4s_x s_t s_{xt} + s_x^2 s_{tt} = 0. \tag{20}$$

Equation (20) can be solved exactly. Its characteristic directions are

$$\frac{\mathrm{d}x}{\mathrm{d}t} = -\frac{3s_t}{s_x}, \qquad \frac{\mathrm{d}x}{\mathrm{d}t} = -\frac{s_t}{s_x},$$

and the Riemann invariants are given by s_t/s_x and s_t/s_x^3, respectively. We define the average horizontal flux by $u = Q/h = -s_t/s_x$. Since u is constant along $\mathrm{d}x/\mathrm{d}t = 3u$,

$$u_t + 3uu_x = 0, \tag{21}$$

which yields

$$u = u_0(x - 3ut), \tag{22}$$

where $u = u_0(x)$ at $t = 0$. At $t = 0$, we prescribe $h(x, 0) = h_0(x)$ and $s(x, 0) = s_0(x)$, and so we have

$$u_0(x) = -\frac{s_{0x} h_0}{2\mu(s_0)}. \tag{23}$$

For given functions s_0, h_0 and μ, Equation (22) defines $u(x, t)$ implicitly. The solvent concentration s then satisfies the first-order equation

$$s_t + us_x = 0, \tag{24}$$

which can, in principle, be solved by the method of characteristics to determine $s(x, t)$ and thence $h(x, t)$. We remark that one of the attractions of this analysis is that it applies when μ is a non-trivial function of s. Note that (22) implies that shocks occur in u if $u_{0x} < 0$ somewhere. In practice we expect some or all of the neglected effects of mean surface tension, gravity, or lateral diffusion of solvent to become significant in these regions of high curvature and act to smooth out the shock.

EXAMPLE SOLUTION

Consider an initial solvent distribution[2] given by $s_0(x) = 4 + 2\cos x$ in an initially uniform layer $h_0(x) = 1$. For simplicity we take $\mu(s) \equiv 1$. Using Equation (23), we obtain $u_0(x) = \sin x$ and so from (22) u is given implicitly by

$$u = \sin(x - 3ut).$$

Hence, there is a unique solution for u until $t = 1/3$, at which time a shock forms. From Equation (24) the solvent concentration s is given by $s = 4 + 2\cos\eta$ where η is given implicitly by

$$t = \frac{|u|^{-3/2}}{2} \int_u^{\sin\eta} \frac{|p|^{1/2}}{(1 - p^2)^{1/2}} \, \mathrm{d}p.$$

In order to clarify the local behaviour of the solution near $x = 0$ we note that $u \sim \xi$ along the characteristics $\xi = x - 3ut \sim x/(1 + 3t) \ll 1$, and hence that $u(x,t) \sim x/(1 + 3t)$ near $x = 0$. Thus,

$$s(x,t) \sim 4 + 2\cos\left[\frac{x}{(1 + 3t)^{1/3}}\right], \qquad h(x,t) \sim \frac{1}{(1 + 3t)^{1/3}}$$

near $x = 0$. A similar analysis can be performed to show that

$$s(x,t) \sim 4 - 2\cos\left[\frac{(\pi - x)}{(1 - 3t)^{1/3}}\right], \qquad h(x,t) \sim \frac{1}{(1 - 3t)^{1/3}}$$

near $x = \pi$. This analysis shows that s_x changes sign at both $x = 0$ and $x = \pi$. As t increases, this change becomes less abrupt near $x = 0$, while near $x = \pi$ the opposite is true and eventually s_x becomes singular at $t = 1/3$. Since negative solvent-concentration gradients drive positive flow, and vice versa, paint flows away from $x = 0$ and towards $x = \pi$. Mass conservation demands that the layer thickness must adjust itself accordingly, so while h decreases gradually at $x = 0$, it increases rapidly at $x = \pi$ and when the driving force s_x becomes singular, then so does h.

In practice, the exact solution for s presented above is difficult to use and so (24) was also solved numerically. The profiles were computed by means of a finite-difference time-marching scheme, based on an explicit time-stepping procedure. Central differences were employed to compute the spatial derivatives, and mass conservation was implicitly built into the numerical scheme. The new solvent distribution and film thickness were updated at each time step. Symmetry boundary conditions were imposed at the endpoints $x = 0, 2\pi$ and once $s(x,t)$ had been computed, $h(x,t)$ was evaluated by means of Equation (19). We also obtained solutions by computing the time evolution of $s(x,t)$ and $h(x,t)$ directly from Equations (8) and (10). Figures 3 and 4 show numerically-calculated values of the layer thickness and solvent concentration, respectively, at $t = 0{\cdot}1, 0{\cdot}2$ and $0{\cdot}3$ and Figure 5 shows the gradient of solvent concentration at $t = 0{\cdot}3$. In particular, Figures 3 and 4 show that the two different numerical methods of obtaining the solutions are in good agreement, while Figure 5 confirms the local behaviour of the solution near $x = 0$ and $x = \pi$ described above.

5. Application to waterborne coatings

The mathematical model developed here for solvent-based high-gloss alkyd paints also applies to other physical situations. For example, it also applies to waterborne coatings (WBCs) which are made up of water, resin and co-solvent. Typically, adding co-solvent lowers the surface tension of the coating, and so, if the co-solvent is more volatile than water (*i.e.* it evaporates faster), it plays the role of the 'solvent' and the remainder of the coating plays the role of the 'resin' in our model with $\Delta\tau > 0$ and hence $M > 0$ as before. In this case we again expect faster initial levelling than in the case where co-solvent is absent and one or more reversals of the free surface profile as the paint dries. Alternatively, if the co-solvent is less volatile than water, the water plays the role of the solvent, but now with $\Delta\tau < 0$ and hence $M < 0$. In this case the present model predicts that the evaporation of the solvent creates surface-tension gradients which resist rather than enhance the levelling. In particular, the analysis in Section 3 shows that this will tend to slow the initial rate of levelling and prevent reversal altogether. All these predictions are in qualitative agreement with recent experimental results [6][3] which
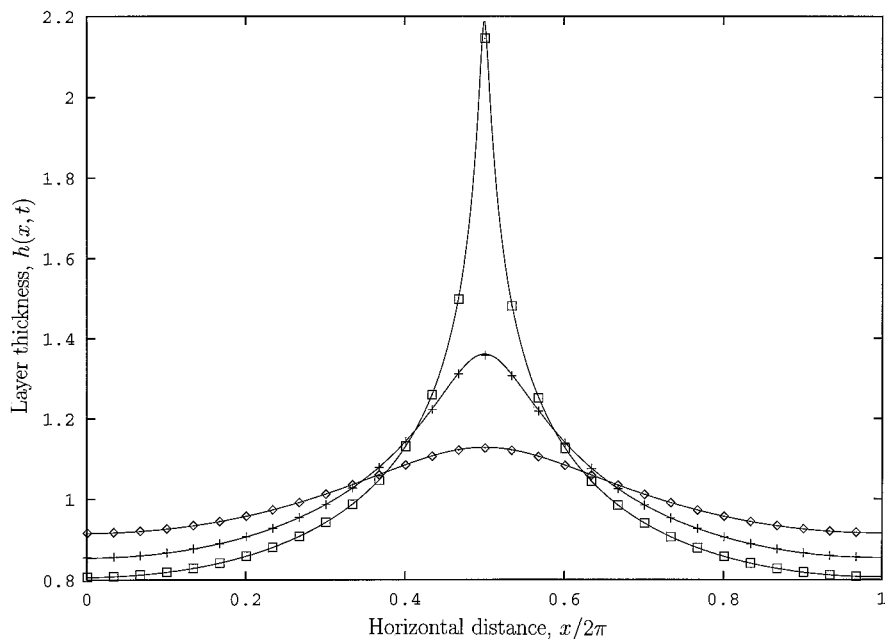
Figure 3. Numerically-calculated values of the layer thickness $h(x, t)$ for purely surface-tension-gradient-driven flow plotted as a function of $x/2\pi$ at time $t = 0{\cdot}1$, $0{\cdot}2$ and $0{\cdot}3$. The symbols denote solutions to Equations (8) and (10), while the solid lines denote solutions calculated from Equations (19) and (24).

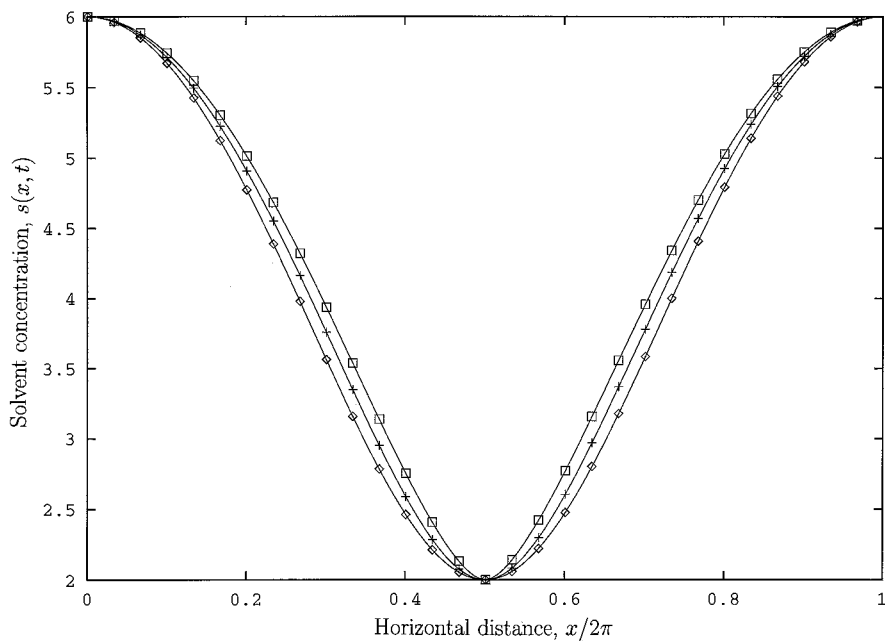*Figure 4.* Numerically-calculated values of the solvent concentration $s(x, t)$ for purely surface-tension-gradient-driven flow plotted as a function of $x/2\pi$ at time $t = 0{\cdot}1$, $0{\cdot}2$ and $0{\cdot}3$. The symbols denote solutions to Equations (8) and (10), while the solid lines denote solutions calculated from Equations (19) and (24).
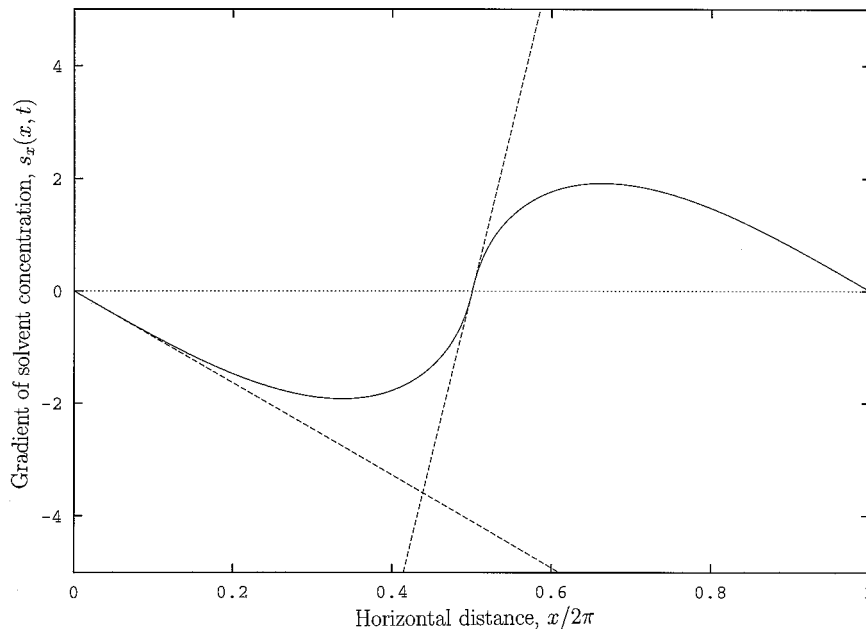
Figure 5. Numerically-calculated values of the gradient of solvent concentration $s_x(x,t)$ for purely surface-tension-gradient-driven flow calculated from Equations (19) and (24) plotted as a function of $x/2\pi$ at time $t = 0{\cdot}3$. The dashed lines show the analytically-calculated asymptotic behaviour of s_x near $x = 0$ and $x = \pi$.

show that a particular waterborne coating with a high volatility co-solvent (specifically WBC/i-BuOH) levels faster than one without co-solvent (WBC/H$_2$O), which itself levels faster than one with a low volatility co-solvent (WBC/EGHE). Furthermore, while the profile of the first coating reverses (twice) during drying, the other two do not reverse at all. Unfortunately, there is insufficient experimental data to permit the quantitative comparison between experiment and theory. However, confirmation that inertia is not the cause of the reversal, as the authors suggest, can be obtained by observing that the reduced Reynolds number for the flow (based on a typical experimental timescale of 5 s) is indeed small, specifically $R = O(10^{-5})$.

6. Conclusions and practical implications

In this paper we have given a systematic derivation of a generalisation of Overdiep's [3, 4] mathematical model for a drying paint layer. The model, which is based on classical lubrication theory and models the paint as consisting of a non-volatile resin and a volatile solvent, was extended to include the effects of variable solvent evaporation rate and solvent diffusivity.

The validity of the model equations depends on the relative sizes of ϵ, the aspect ratio of the layer, and D, the dimensionless parameter which measures the importance of solvent diffusion to solvent convection. When $\epsilon^2 \ll D \ll 1$, the model of Overdiep [3] is recovered. If $D \sim 1$, the model is modified to include lateral diffusion of solvent as suggested by Overdiep [4]. When $D \gg 1$, lateral diffusion of solvent dominates the flow, while, if the condition $D \gg \epsilon^2$ fails to hold, the leading-order distribution of solvent across the layer is no longer uniform. In both these latter two cases Overdiep's [3, 4] model is no longer valid. Thus, we have shown that the models derived by previous authors are applicable, provided that the ratio of solvent diffusion to solvent convection is neither too large nor too small. In particular, this means that

the horizontal lengthscale of the flow (given, for example, by the lengthscale of the initial perturbation to a uniform layer) must satisfy

$$L \gg \left(\frac{H^5 \tau_r}{D_0 M_0} \right)^{1/4}$$

for mean surface-tension-dominated flow or

$$L \gg \left(\frac{H^3 S \Delta \tau}{D_0 M_0} \right)^{1/2}$$

for surface-tension-gradient-dominated flow. As we have already observed, the diffusivity of solvent may decrease by several orders of magnitude as the solvent concentration decreases from 1 to 0, suggesting that the models may become invalid at low solvent concentrations. In practice, however, the decrease in diffusivity with solvent concentration may be accompanied by a rapid increase in the viscosity. This will mean that the drop in the effective diffusivity (accounting for the change in the viscosity) may not be as large as the drop in the diffusivity and so the models may actually apply over the whole range of solvent concentrations.

We also analysed the evolution of small perturbations to the thickness of, and the concentration of solvent in, a drying paint layer. The results show that surface-tension-gradient effects result in a faster initial levelling rate than that due solely to mean surface-tension effects and can cause an initial perturbation to the profile layer to reverse (*i.e.* peaks become troughs and vice versa) one or more times. They also show that an initially flat free surface can become perturbed if the solvent concentration is not initially uniform. In particular, the results show that surface-tension-gradient effects alone are sufficient to explain all these phenomena. This issue has been discussed by several previous authors. For example, in a recent experimental paper [5] describing the levelling of various waterborne coatings, while acknowledging the importance of surface-tension-gradient effects, it is stated that 'The reappearance of surface ripples cannot be explained without the effects of inertia ...'. The present work clearly shows that, while other factors such as variations in viscosity during drying, non-uniform solvent evaporation and non-uniform solvent diffusivity (all of which are included in the present model) and fluid inertia (which is negligible in all but the most extreme practical situations) can, of course, affect the progress of levelling, none is required to explain the observed reversal behaviour satisfactorily.

In some circumstances the flow is initially dominated by surface-tension-gradient effects. In these situations the governing equations simplify to a single quasi-linear second-order hyperbolic equation which can be solved analytically as well as numerically. The solutions thus obtained clearly show that surface-tension-gradient effects can produce regions of high curvature in the thickness of even an initially flat layer, once again emphasising the importance of achieving uniform solvent distributions at the beginning of the drying process.

Finally, we showed how the present model can also be applied to waterborne coatings. Although a quantitative comparison between theory and experiment was impossible in this case, we were able to show that the qualitative agreement between the two is excellent.

In conclusion, we note that the present model also applies to other industrial situations involving thin coatings consisting of volatile and non-volatile components with different surface tensions, such as, for example, the manufacture of electrical components.

Acknowledgements

Appendix

Motivated by the results listed in Table 2 which show that the parameter E is typically small, in this Appendix we obtain the asymptotic solution of Equation (13) in the limit of small non-dimensional evaporation rate, $E \to 0$. Following the approach of Wilson [8], we seek solutions for $h_1(t)$ and $s_1(t)$ in the forms

$$h_1(t) = h_{10}(t) + Eh_{11}(t) + O(E^2), \quad s_1(t) = s_{10}(t) + Es_{11}(t) + O(E^2).$$

Clearly, this expansion scheme is only useful provided that

$$t \ll \frac{1}{E} \min\left(1, \frac{1}{(1-S_0)}, \frac{1}{M_1(1-S_0)}\right),$$

where $M_1 = -\mathrm{d}\mu/\mathrm{d}s|_{s=S_0}$. At leading order in E, (12) yields

$$s_{10} = S_1 \, \mathrm{e}^{-\alpha^2 Dt}, \tag{A1}$$

while (13) gives

$$h_{10t} + \sigma h_{10} + \gamma S_1 \, \mathrm{e}^{-\alpha^2 Dt} = 0, \tag{A2}$$

and so

$$h_{10} = \left(H_1 + \frac{\gamma S_1}{\sigma - \alpha^2 D}\right) \mathrm{e}^{-\sigma t} - \frac{\gamma S_1}{\sigma - \alpha^2 D} \mathrm{e}^{-\alpha^2 Dt}. \tag{A3}$$

At first order, (12) yields

$$s_{11} = S_1 \left(1 - \frac{\gamma(1-S_0)}{\sigma - \alpha^2 D}\right) t \, \mathrm{e}^{-\alpha^2 Dt} + \frac{1-S_0}{\sigma - \alpha^2 D}\left(H_1 + \frac{\gamma S_1}{\sigma - \alpha^2 D}\right)(\mathrm{e}^{-\alpha^2 Dt} - \mathrm{e}^{-\sigma t}), \tag{A4}$$

while (13) gives

$$h_{11t} + \sigma h_{11} + (\bar{A}t + \bar{B}) \, \mathrm{e}^{-\sigma t} + (\bar{C}t + \bar{D}) \, \mathrm{e}^{-\alpha^2 Dt} = 0, \tag{A5}$$

where the constants $\bar{A}, \bar{B}, \bar{C}$ and $\bar{D}$ are given by

$$\bar{A} = -\sigma(3 + M_1(1 - S_0))\left(H_1 + \frac{\gamma S_1}{\sigma - \alpha^2 D}\right),$$

$$\bar{B} = -\frac{\gamma(1 - S_0)}{\sigma - \alpha^2 D}\left(H_1 + \frac{\gamma S_1}{\sigma - \alpha^2 D}\right),$$

$$\bar{C} = \frac{\gamma S_1}{\sigma - \alpha^2 D}(2\sigma + \alpha^2 D + (\alpha^2 D M_1 - \gamma)(1 - S_0)),$$

$$\bar{D} = \frac{\gamma(1 - S_0)}{\sigma - \alpha^2 D}\left(H_1 + \frac{\gamma S_1}{\sigma - \alpha^2 D}\right).$$

The solution to Equation (A5) has the form

$$h_{11} = (\bar{a}t^2 + \bar{b}t + \bar{c})\,\mathrm{e}^{-\sigma t} + (\bar{d}t + \bar{e})\,\mathrm{e}^{-\alpha^2 Dt}, \tag{A6}$$

where

$$\bar{a} = -\frac{\bar{A}}{2}, \qquad \bar{b} = -\bar{B}, \qquad \bar{c} = -\bar{e} = \frac{(\sigma - \alpha^2 D)\bar{D} - \bar{C}}{(\sigma - \alpha^2 D)^2}, \qquad \bar{d} = -\frac{\bar{C}}{\sigma - \alpha^2 D},$$

are constants. These solutions clearly show that when $D \sim 1$ diffusion eventually dominates and all perturbations die out as t becomes large[4]. However, when lateral diffusion of solvent is dominated by convection ($\epsilon^2 \ll D \ll 1$), we obtain the corresponding solutions by setting $D = 0$ in the above expressions and their behaviour is rather more interesting. (Note that setting $D = 0$ in these expression does *not* mean that $D = 0$, but simply that $D \ll 1$.) Equations (A1) and (A3) show that in this case at leading order the perturbation to the solvent concentration is unaltered, while, as t becomes large, the perturbation to the free surface ultimately has amplitude $-\gamma S_1/\sigma = -3MS_1/2(\alpha^2 C + B)$. Equations (A4) and (A6) show that the long-time behaviour of s_{11} and h_{11} depends crucially on whether $S_1 = 0$ or $S_1 \neq 0$. If $S_1 = 0$ then as t becomes large

$$s_{11} \to \frac{(1 - S_0)H_1}{\sigma} = \frac{3(1 - S_0)H_1}{\alpha^2(\alpha^2 C + B)},$$

$$h_{11} \to -\frac{\gamma(1 - S_0)H_1}{\sigma^2} = -\frac{9M(1 - S_0)H_1}{2\alpha^2(\alpha^2 C + B)^2},$$

the latter expression representing the reversal of the initial perturbation to the free surface and the former the appearance of a corresponding perturbation to the solvent concentration. Alternatively, if $S_1 \neq 0$ then as t becomes large

$$s_{11} \sim S_1\left(1 - \frac{\gamma(1 - S_0)}{\sigma}\right)t = S_1\left(1 - \frac{3M(1 - S_0)}{2(\alpha^2 C + B)}\right)t,$$

$$h_{11} \sim -\frac{\gamma S_1}{\sigma}\left(2 - \frac{\gamma(1 - S_0)}{\sigma}\right)t = -\frac{3MS_1}{2(\alpha^2 C + B)}\left(2 - \frac{3M(1 - S_0)}{2(\alpha^2 C + B)}\right)t,$$

so ultimately $|s_{11}|$ and $|h_{11}|$ both grow linearly in time and eventually they become so large that the expansion scheme fails.

Notes

[1] Notice that because the surface tension is given by $\tau(s) = 1 - \epsilon^2 M s_0/C + o(\epsilon^2)$, it contributes only a constant to the leading-order normal-stress condition (6). Overdiep [3, 4] and Wilson [8] both incorrectly retained higher-order terms arising from the variation in the surface tension in this boundary condition.

[2] In the case of purely surface-tension-gradient-driven flow we have the freedom to rescale s arbitrarily, and have done so here to simplify the presentation that follows.

[3] Note that in Figure 1 of this paper the experimental points are incorrectly labelled.

[4] More precisely this means that t satisfies $\max(\sigma^{-1}, \alpha^{-2}D^{-1}) \ll t \ll S_0/E$.

References

1. N.P.D. Smith, S.E. Orchard and A.J. Rhind-Tutt, The physics of brush marks. *J. Oil and Colour Chemists' Assoc.* 44 (1961) 618–633.
2. S.E. Orchard, On surface levelling in viscous liquids and gels. *Appl. Sci. Res. A* 11 (1962) 451–464.
3. W.S. Overdiep, Levelling of paints. In: D.B. Spalding (ed.) *Physiochemical Hydrodynamics, V.G. Levich Festschrift, Vol. 2.* London: Advance Publications Limited (1978) pp. 683–697.
4. W.S. Overdiep, The levelling of paints. *Prog. in Org. Coatings* 14 (1986) 159–175.
5. S. Kojima, T. Moriga and K. Takenouchi, The leveling of thermosetting waterborne coatings. Part 1: Observation of leveling process. *Polym. Eng. Sci.* 33 (1993) 1320–1328.
6. S. Kojima, T. Moriga and K. Takenouchi, The leveling of thermosetting waterborne coatings. Part 3: Leveling under controlled conditions. *Polym. Eng. Sci.* 35 (1995) 1949–1954.
7. L.O. Kornum and H.K. Raaschou Nielsen, Surface defects in drying paint films. *Prog. in Org. Coatings* 8 (1980) 275–324.
8. S.K. Wilson, The levelling of paint films. *IMA J. Appl. Math.* 50 (1993) 149–166.
9. J.A. Moriarty, E.L. Terrill and S.K. Wilson, Mathematical modelling of drying paint layers. In: H. Neunzert (ed.) *Progress in Industrial Mathematics at ECMI 94.* Chichester and Stuttgart: John Wiley and Sons Limited and B.G. Teubner (1996) pp. 112–119.
10. L.W. Schwartz and R.R. Eley, Numerical simulation of post-application coating flows, including flows arising from surface-tension gradients. Unpublished manuscript.
11. D.E. Weidner, L.W. Schwartz and R.R. Eley, Role of surface tension gradients in correcting defects in corners. *J. Coll. Interf. Sci.* 179 (1996) 66–75.
12. J.P. Burelbach, S.G. Bankoff and S.H. Davis, Nonlinear stability of evaporating/condensing liquid films. *J. Fluid Mech.* 195 (1988) 463–494.
13. O.E. Jensen and J.B. Grotberg, Insoluble surfactant spreading on a thin viscous film: shock evolution and film rupture. *J. Fluid Mech.* 240 (1992) 259–288.
14. O.E. Jensen and J.B. Grotberg, The spreading of heat or soluble surfactant along a thin liquid film. *Phys. Fluids A* 5 (1993) 58–68.
15. A. De Wit, S. Gallez and C.I. Christov, Nonlinear evolution equations for thin liquid films with insoluble surfactants. *Phys. Fluids* 6 (1994) 3256–3266.
16. R. van der Hout, Personal communication. (1992).